Environmental Science and Pollution Research (2022) 29:51732–51743
https://doi.org/10.1007/s11356-021-17568-2

RESEARCH ARTICLE

Noble metal-doped TiO_2 thin films in the efficient removal of Mordant Orange-1: insights of degradation process

Chhakchhuak Vanlalhmingmawia[1] · Chhakchhuak Lalhriatpuia[2] · Diwakar Tiwari[1] · Dong-Jin Kim[3]

Received: 1 July 2021 / Accepted: 12 November 2021 / Published online: 5 March 2022

Abstract

Nanocomposite Ag^0(NPs)/TiO_2 is synthesised in a facile template method enabling nanoparticles of reduced Ag evenly distributed within the titania network. The morphological studies of nanocomposites were extensively performed employing SEM/EDX (scanning electron microscopy/energy dispersive X-ray), TEM (transmission electron microscopy) and AFM (atomic force microscopy). Moreover, the bandgap energies of materials were obtained using the diffuse reflectance spectrometer (DRS). The newer insights in the photocatalytic elimination of Mordant Orange-1 (MO1) was obtained using the nanocomposite thin film for various parametric studies utilising the UV-A and LED illuminations. The kinetics of degradation of MO1 was performed, and the rate constant was favoured at lower concentrations of MO1. Moreover, the elimination efficiency of MO1 was favoured with a decrease in solution pH. The NPOC results inferred that a fairly good extent of MO1 was mineralised using a thin-film catalyst for both the UV-A and LED illuminations. The minimal effect of several co-ions demonstrated the applicability of thin films in the elimination of MO1, and the stability of the thin film has shown the potential applicability of thin-film catalysts. Further, the mechanism of photocatalytic degradation was demonstrated with the radical scavenger studies and ascertained the reaction pathways.

Keywords Insights of degradation · Kinetic studies · Mineralisation of Mordant Orange-1 · Mordant Orange-1 · Nanocomposite · Surface plasmon resonance

Introduction

The contamination of aquatic environments with innumerable dye compounds is a greater environmental concern. Several dyes, dye precursors are seemingly known as carcinogenic/mutagenic (Matouq et al. 2014). The main entry route of synthetic dyes in water bodies is through the effluent discharged from the industries viz., textile, paper, leather, paint, food, cosmetics, pharmaceuticals, hair colourings, etc. (Verma et al. 2012; Papić et al. 2004). It was reported that the annual dye production exceeds 7×10^5 tons (Lee et al. 2006; Riera-Torres et al. 2010), and nearly 10–15% of the total dyes are directly entering through the effluents during the synthesis and dyeing processes (Husain 2006; Gupta and Suhas 2009; Hai et al. 2007). Moreover, textile dyes estimated at around 2.8×10^5 tons are eventually released into the water bodies through the industrial effluents every year (Jin et al. 2007; H et al. 2017). Synthetic dyes are refractory in nature as they are trivially biodegradable in nature and are known to be highly stable against some oxidising agents (Sadeghzade-Attar 2018). Hence, such dyes are often escaped from the current wastewater treatment plants and entered into the water bodies which caused serious and adverse effects to the aquatic environment (Jung et al. 2016; Su et al. 2011; Muhd Julkapli et al. 2014). Azo dye compounds are known to be highly toxic causing several health issues such as allergy, skin diseases, cancer, defect in embryo development, etc. (Rosu et al. 2017; Alves de Lima et al. 2007; Hatch and Maibach 1995). Therefore, complete and efficient removal of dye compounds from the water

Responsible Editor: Sami Rtimi

✉ Diwakar Tiwari
Ediw_tiwari@yahoo.com

[1] Department of Chemistry, School of Physical Sciences, Mizoram University, Aizawl 796004, India

[2] Department of Chemistry, Pachhunga University College, Mizoram University, Aizawl 796001, India

[3] Department of Environment Science and Biotechnology, Hallym University, Chuncheon 24252, Republic of Korea

bodies is a greater need for the existing treatment plants (Yagub et al. 2014).

Mordant Orange-1 (MO1) dye is an azo dye having a complex aromatic structure and is highly stable in nature. It is synthesised by the diazo coupling reaction, and these compounds are not degraded efficiently with the conventional wastewater treatment plants (Abdel-Messih et al. 2013). Therefore, several methods are assessed for the removal of MO1 viz., adsorption (Li et al. 2018; Salama 2017), coagulation (Shi et al. 2007; Li et al. 2016; Kuppusamy et al. 2017), foam separation (Schwarze et al. 2017), biological treatment, etc. (Paz et al. 2017; Shen et al. 2018). However, the existing water treatment plants showed an additional environmental burden because it releases large amounts of sludge (Gracia-Lor et al. 2012). However, the commonly used chemical oxidants viz., chlorine, hypochlorite, and ozone are widely employed because of their easy availability, cost-effectiveness, and possible efficiency. Although the use of these oxidants is based on the 'no waste' process it causes, in cases, the formation of harmful by-products or sometimes inadequate efficiency in particular towards the calcitrant chemicals. Moreover, the chlorination and ozonation are accompanied by the formation of harmful disinfection by-products (DBPs) viz., hypohalous compounds (Krasner et al. 2009). These by-products are potential mutagens or carcinogens and are even more harmful compared to the parent compounds.

On the other hand, the advanced oxidation process (AOPs) using heterogeneous TiO_2 photocatalysis is a highly efficient and relatively greener treatment process to be employed in wastewater treatments. The principle of AOPs lies in the in situ formation of reactive hydroxyl radicals which readily oxidises even persistent compounds in aqueous wastes. Further, widespread use of TiO_2 as the heterogeneous catalyst is because of its unique properties viz., excellent thermal and chemical stability, biocompatibility, low toxicity, low cost, easy fabrication, engineered material, etc. However, the bare titanium dioxide possessed a wide bandgap energy and showed a rapid charge recombination rate which restricted its implications in the treatment processes. Therefore, alternatively, the doping of titanium dioxide with a nonmetal, transition metal, or noble metal reduces significantly the bandgap energy which allows readily to absorb visible light (Mogal et al. 2014). The doped titanium dioxide shows an enhanced reactivity in the photocatalytic processes using visible light or even to harness the solar radiations (Ge et al. 2006). Fluorinated-titanium dioxide (TiO_2-F) nanoparticles in the form of anatase polymorph and fluorinated and/or N-doped TiO_2 nanopowders show an efficient photocatalytic disinfection performance for the bacteria, *Escherichia coli* (*E. coli*) under visible light irradiation in an aqueous medium (Milosevic et al. 2017; Milošević et al. 2018).

The noble metals (Ag, Au, Pd, and Pt) show unusually high Schottky barriers which help to trap electrons and reduce electron–hole pair recombination. They also exhibit the surface plasmon resonance (SPR) effect which enables titanium dioxide catalysts to absorb light at the visible region and enhances the excitation of electrons and enhances the photocatalytic efficiency (Selvaraj and Li 2006) (Zangeneh et al. 2015). Silver (Ag) nanoparticles show an enormously intense SPR effect at the wavelength of 320–450 nm near the bandgap energy of titanium dioxide (~3.2 eV, 388 nm). In Ag^0 TiO_2 photocatalyst, the movement of electrons between the conduction band of titanium dioxide and Ag nanoparticles is favourable since the Fermi level of silver metal is lower as compared to the titanium dioxide (Selvaraj and Li 2006). This causes the generation of Schottky barriers within the metal–semiconductor which helps excited electrons to move towards the electric field and the holes towards the opposite direction of the electric field. This inhibits the fast electron–hole pair recombination (Liu et al. 2013; Lee et al. 2006). Ag-decorated TiO_2-nanotube was successfully utilised for the adhesion and inactivation of *Escherichia coli* under visible light (Hajjaji et al. 2018). The photocatalytic process enabled the removal of 100% of chloramphenicol just within 20 min under optimum conditions, and about 88% TOC (total organic carbon) was removed after 120 min of treatment (Shokri et al. 2013; Zhang et al. 2010). Therefore, the Ag^0(NP)/TiO_2 is a promising photocatalyst for a variety of photocatalytic reactions (Z et al. 2014; Sofianos et al. 2014; Tiwari et al. 2018, 2020). The doping of noble metal nanoparticles within the TiO_2 network often leads to agglomeration which greatly affects the catalytic action. Therefore, the communication deals with a suitable template synthesis of titanium dioxide with in situ and facile doping of Ag^0(NP) to the titanium dioxide crystal structure. Moreover, the thin film of Ag^0(NPs)/ TiO_2 (nanocomposite) was obtained by a simple dip coating process. The insight of the catalytic activity of thin films was conducted in the elimination of Mordant Orange-1 in aqueous wastes using UV-A and LED light illuminations.

Materials and methods

Chemicals used

$Ti[OCH(CH_3)_2]_4$ (97.0%), $AgSO_4$, CH_3COOH, $NaBH_4$, polyethylene glycol (PEG), and Mordant Orange-1 are the product of Sigma Aldrich. Co., USA. Ethylenediamine tetraacetate (98.0%) and glacial acetic acid are obtained from Loba Chemie, India. Ethanol (anhydrous) (99.9%) is procured from Changshu Yangyuan Chemical, China. NaCl (99.0%), NaN_3 (99.0%), oxalic acid dihydrate (99.0%), 2-propanol (99.7%), $NiCl_2$ (95.0%), $CuSO_4$ (99.0%), glycine (99.9%),

and $NaNO_3$ are products of Merck India Ltd., India. Purified water is collected from Sartorius Water Purification System (model: Arium mini plus UV Lab., Sterile Plus, Sartopore 2150, Germany; pore size of 0.45 + 0.2 mm). The real water sample is obtained from the Reiek Kai site of the Tlawng River, near Aizawl city (India). A spectrophotometer (UV-1800, Shimadzu, Japan) is employed for measuring the absorbance data of MO1.

Standard MO1 (50.0 mg/L) solution is prepared carefully in distilled water. The stock solution of MO1 is diluted to obtain various concentrations of MO1 viz., 0.5, 1.0, 5.0, 10.0, 15.0, and 20.0 mg/L and utilised for obtaining the calibration line. The λ_{max} 371.5 nm is obtained for MO1. The degradation kinetics of MO1 was conducted obtaining the concentrations of MO1 at various time intervals. The TOC (Shimadzu, Japan; model: TOC-VCPH/CPN) Analyser is used in analysing the apparent mineralisation of MO1.

Methodology

Preparation of Ag^0(NPs)/TiO_2 thin film

The Ag^0(NP) are obtained by a simple reduction process (Rashid et al. 2013; Lalliansanga et al. 2019). Further, the nanocomposite Ag^0(NPs)/TiO_2 is obtained by a facile sol–gel synthetic route. Polyethylene glycol (PEG) was used as a support for making a mechanically stable TiO_2 film and to induce a strong adhesion. This will prevent the catalyst from leaching out after the repeated photocatalytic cycles (Rtimi et al. 2013). A total of 2.92 mL of titanium isopropoxide $Ti[OCH(CH_3)_2]_4$ (TISP) and 2.0 g of poly(ethylene glycol) (PEG) were added to 1.3 mL acetyl-acetone (AcAc). Instantly, 10.0 mL of freshly prepared Ag^0(NP) solution was dispersed to the solution mixture. The titanium solution was gently mixed with a solution mixture of 23.3 mL ethanol (EtOH), 0.55 mL acetic acid (AcOH), and 2.25 mL distilled water (H_2O). This results in the initiation of hydrolysis and condensation reactions. The resulting Ag^0(NPs)/TiO_2 solution mixture was vigorously stirred for 2 h. Then, the sol solution was sonicated for 30 min in a sonication bath. The sol solution was collected; it was then left for around 24 h for ageing before being used for making the thin film photocatalyst. Further, the thin films were fabricated as defined elsewhere (Tiwari et al. 2018, 2020).

Characterisation of the thin film

Ag^0(NPs)/TiO_2 thin film was characterised by the SEM (model: FE-SEM SU-70, Hitachi, Japan) images. Further, high-resolution structural images are obtained using the TEM (Tecnai F20 transmission electron microscope, FEI, USA) analyser. AFM (XE-100 apparatus from Park Systems, Korea) images give the 3D topographical images of nanocomposite thin films. The DRS data were obtained using the UV–VIS-NIR spectrophotometer (Evolution 220; Thermo Scientific). The data were recorded at a bandwidth of 1 nm over a wavelength range of 200 to 800 nm.

Reactor operation in the degradation of Mordant Orange-1

The concentration-dependent studies are conducted by varying the initial concentrations of MO1 from 0.5 to 20.0 mg/L, and pH is adjusted using 1.0 mol/L HCl/NaOH. The photocatalytic elimination of MO1 is performed in a self-assembled black box. The pollutant solution (50 mL) is taken inside the black box. Nanocomposite thin film is taken inside the reactor vessel. UV-A illumination having λ_{max} of 360 nm (model: 9 W, PLS9 W BLB/2 P 1CT, Philips) or a visible LED light (Havells LED Adore 20 W, India) was placed *Ca* 12 cm above to dye solution. This provides the light-radiation passes through the dye solution and reaches the thin film photocatalyst surface. This leads to initiate the photocatalytic degradation of MO1 at the thin film surface. A self-assembled water bath keeps the reactor temperature (24 ± 1 °C). The treated solution of MO1 is analysed by UV–Vis spectrophotometer at certain time intervals maximum up to 2 h of photo-illumination. Further, the blank experiment is conducted to use only UV-A or LED light illuminations in the absence of thin-film photocatalyst.

Results and discussion

Characterisation of thin film

SEM micrographs of Ag^0(NP)/TiO_2 are shown in Fig. 1a. The result showed that small-sized TiO_2 particles are distributed uniformly onto the silicate glass and form a uniform thin film of the nanocomposite. However, at places, cracks are observed on the surface. Further, it is interesting to observe that the titanium dioxide is not agglomerated on the surface. This is because of the template synthesis to titania. The EDX analysis of the thin film sample was conducted and shown in Fig. 1a (inset). It is evident from the figure that the silver nanoparticles are incorporated within the titania network. Similarly, the TEM image of the nanocomposite is shown in Fig. 1b. The high-resolution TEM image clearly showed the fringes of Ag nanoparticles, and it is uniformly distributed with TiO_2 structure. Moreover, the interplanar distance of the Ag^0(NP) is estimated as 0.15 nm.

Similarly, the AFM image of nanocomposite thin film is shown in Fig. 1c. The AFM image inferred that the surface of the thin film of photocatalyst is highly uneven or heterogeneous in nature and it possessed small-sized

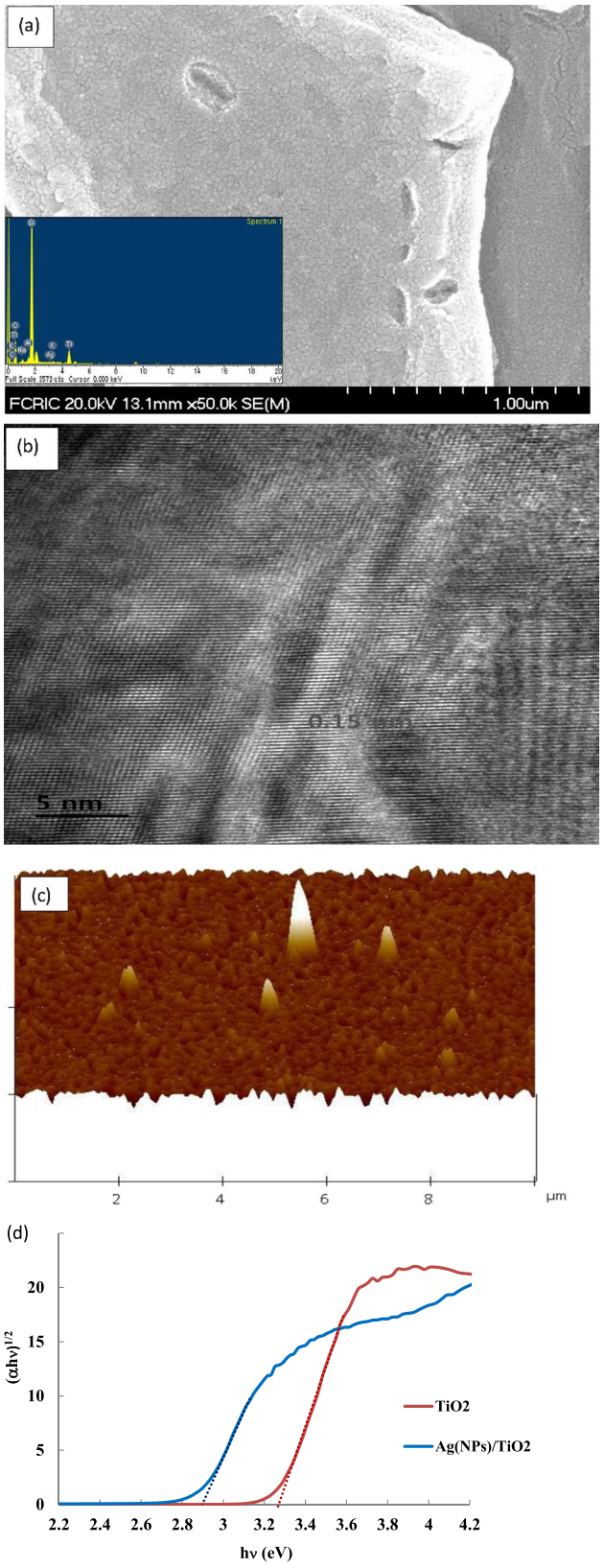

Fig. 1 Morphological studies of the nanocomposite material. **a** SEM image of the thin film; **b** TEM image of the Ag^0(NPs)/TiO_2 nanocomposite; **c** AFM image of the thin film (Scale X: 2 µm/div; Z: 350 µm/div and data scale 350 nm); and **d** Tauc plot for bare TiO_2 and Ag^0(NPs)/TiO_2 powder samples

pillars of titanium dioxide having a maximum height of ca. 350 nm. Further, the root mean square roughness (R_q) and mean roughness (R_a) of the thin film was 16.952 nm and 12.250 nm, respectively.

Diffuse reflectance spectra (DRS) of powder TiO_2 and Ag^0(NPs)/TiO_2 was obtained using a UV–Vis spectrophotometer. The bandgap energy of the material was calculated by converting the diffuse reflectance data into its absorption coefficient (α) values using the Kubelka–Munk equation and plotting the graph using Tauc's relation (Sangiorgi et al. 2017). The resulting Tauc plot is shown in Fig. 1d. The bandgap energies for TiO_2 and Ag^0(NPs)/TiO_2 were determined to be 3.28 and 2.9 eV, respectively. This clearly indicates that the presence of Ag^0(NPs) greatly reduced the bandgap energy of the nanocomposite material.

Photocatalytic removal of MO1

pH dependence removal

The effect of pH is a useful parameter that demonstrates the mechanism of photocatalytic elimination of pollutants. This is mainly due to the pH dependence transitions in pollutant species as well as the surface properties of active sites of photocatalysts (Lalhriatpuia et al. 2015). Therefore, the pH influenced the overall efficiency of the photocatalyst in the degradation of pollutant molecules (Zucca et al. 2008). The photocatalytic elimination of MO1 is carried out for a wide range of pH (4.0–10.0) and results are depicted in Fig. 2. The percentage removal of the MO1 was obtained after the 2-h irradiation. Results clearly showed that the decrease in pH, i.e. pH 10.0 to 4.0 has caused an increase in the elimination of MO1. Quantitatively, with a decrease in solution pH from 10.0 to 4.0, the corresponding increase in percent removal of MO1 is from 29.15 to 61.3% (for UV-A) and 16.65 to 35.81% (for LED light) using nanocomposite thin film photocatalyst. The MO1 molecule contains two dissociable hydrogens, one from the carboxylic group and the second is due to the phenolic group which have the pk_a values of 5.0 and 11.0 (Nazar et al. 2010). Therefore, within the pH region 6.0–10.0, the MO1 molecule usually exists as monoanionic species. However, the phenolic and carboxylic groups forming the hydrogen bonding result in a nonionic species. Hence, in this pH range, the MO1 molecule exists in equilibrium between the monoanionic species (cf Fig. 2 (inset)) (Nazar et al. 2010). Further, pH > 10.0, both the protons of the MO1 molecule are dissociated; hence, the monoanionic MO1 molecule becomes dianionic species. Thus, the net charge of the MO1 species greatly becomes negative at and above pH 10.0. On the other hand, the pH_{pzc} of nanocomposite was obtained to be 6.8 (Tiwari et al. 2020). This infers that the thin

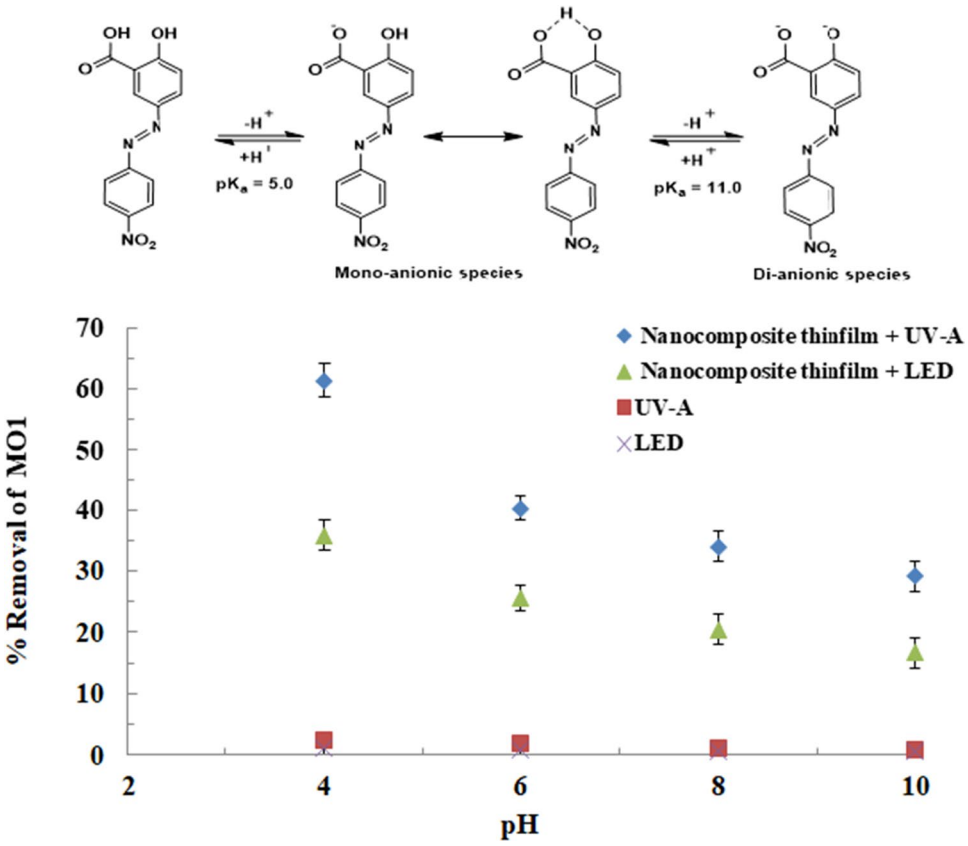

Fig. 2 Percentage elimination of MO1 with the effect of solution pH [initial concentration of MO1: 5.0 mg/L] and the inset of the equilibrium of MO1 as a function of pH

film possesses a net positive charge at pH < 6.8 whereas its surface possesses negative charges at pH > 6.8. These studies showed that increasing the pH gradually enhances the net negative charges both on the nanocomposite surface and MO1 species. This eventually caused enhanced Coulombic repulsions between the MO1 species and nanocomposite surface which resulted in the gradual decrease of MO1 removal at pH > 6.0 (pH 6 ~ 10). Photocatalytic removal of Alizarin Yellow using the catalyst Au^0(NPs)/TiO_2 thin film showed similar trends (Lalliansanga et al. 2019). Copper-deposited TiO_2 nanoparticles (Cu_2O-CuO/TiO_2) were prepared using a combination of impregnation and precipitation-deposition method was also successfully utilised for the pH-dependent photocatalytic degradation of commercial dyes such as Reactive Blue 49 (RB 49), Reactive Red 24 (RR 24), and Reactive Yellow 160 (RY 160) under UV irradiation (Ajmal et al. 2016). Further, the reaction was conducted employing UV-A and LED illuminations without using nanocomposite thin films at a wide range of pH (pH 4.0–10.0). It was observed that a negligible amount of MO1 was degraded after 2 h of contact. These results clearly inferred that the nanocomposite catalyst greatly favoured the elimination of MO1 in aqueous media by UV-A or LED lights. Further, compared to the UV-A and LED light illumination, the UV-A light showed a relatively higher degradation of MO1 throughout the studied pH.

Concentration dependence removal of MO1

Concentration dependence elimination of MO1 is analysed for varied concentrations of MO1 (0.5–20.0 mg/L; pH 6.0). The removal efficiency of MO1 is illustrated in Fig. 3. Figure 3 demonstrates that the decrease in concentration greatly favoured the removal efficiency of MO1. The decreasing

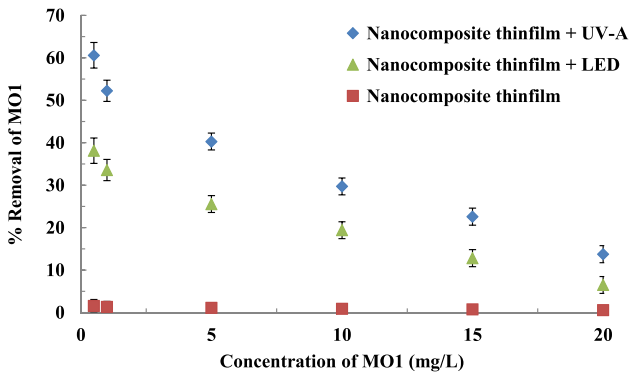

Fig. 3 Removal efficiency of MO1 as a function of the concentration of MO1 [pH of solution: 6.0]

concentration of MO1 from 20.0 to 0.5 mg/L had enabled to increase the percentage degradation of MO1 from 13.7 to 60.6% (for UV-A) and 6.5 to 38.14% (LED light), respectively. The decrease in degradation efficiency with an increase in the concentration of MO1 is, perhaps, due to the reason that the contact possibility of MO1 at the photocatalyst surface was relatively less at a higher concentration of MO1 dye (Tiwari et al. 2015). It is also evident that at a high concentration of MO1, the scavenging effect increases which possibly results in a decrease in the percentage removal of the MO1 (Nasseri et al. 2017). These results are in a line with the result obtained in the photocatalytic degradation of Reactive Green 12 (RG 12) using TiO_2 impregnated polyester in which the dye removal was significantly reduced with an increase in RG 12 concentration. Here, at a lower concentration of RG 12, the solution transparency was comparatively more which enables enhanced penetration of light on the photocatalyst surface. This causes to generate enhanced active species (Hichem et al. 2017). Furthermore, a dark reaction is performed employing the catalyst Ag^0(NPs)/TiO_2 at various concentrations of MO1 (0.5–20.0 mg/L; pH 6.0). It was observed that almost a negligible amount of MO1 was removed even after 12 h of contact. Therefore, this indicates that no surface adsorption is taking place using the nanocomposite thin film at least for MO1.

Kinetic study of MO1 degradation

The time dependence kinetics is carried out to assess the performance of nanocomposite photocatalyst in the elimination of MO1. The kinetic results obtained at varied concentrations of MO1 is shown in Table 1. It is observed that degradation of MO1 proceeds through a pseudo-first-order rate equation (Lalliansanga et al. 2019). Further, the time-dependent degradation kinetics of MO1 is favoured with the dilution, i.e. increasing the concentration of the dye results in the decrease of rate constant values. Moreover, the rate of degradation of MO1 is faster using UV-A light irradiations compared to LED light irradiations. Similar data is reported earlier where methylene blue was degraded using graphene-decorated TiO_2 (Acosta-Esparza et al. 2020).

Additionally, the removal of MO1 is modelled to the Langmuir–Hinshelwood (L–H) rate kinetics using the standard equations (Lalliansanga et al. 2019). The Langmuir–Hinshelwood (L–H) adsorption constant (k_r; mg/L/min) and the reaction rate constant (K; L/mg) are computed as 0.038 and 0.202 (R^2: 0.997 for UV-A) and 0.018 and 0.255 (R^2: 0.976 for LED), respectively.

Table 1 Pseudo-first-order rate constants in the photocatalytic removal of MO1 employing nanocomposite thin film employed under UV-A and LED light irradiations [pH of solution: 6.0]

Initial concentration of MO1 (mg/L)	UV-A irradiation		LED light irradiation	
	Rate constant $k_1 \times 10^{-3}$	R^2	Rate constant $k_1 \times 10^{-3}$	R^2
0.5	7.0 ± 0.9	0.965	4.1 ± 0.5	0.998
1.0	5.9 ± 0.7	0.993	3.4 ± 0.4	0.982
5.0	4.0 ± 0.6	0.987	2.5 ± 0.4	0.999
10.0	2.9 ± 0.4	0.989	1.8 ± 0.3	0.998
15.0	2.0 ± 0.5	0.979	1.1 ± 0.3	0.995
20.0	1.4 ± 0.3	0.952	0.5 ± 0.1	0.994

Mineralisation of MO1

The extent of mineralisation of pollutants in the photocatalytic treatment demonstrates the efficiency of operation. The percentage mineralisation of MO1 is obtained at a wide range of pollutant concentrations (1.0 to 20.0 mg/L; pH ~ 6.0). Results are shown in Fig. 4a. Results indicated that a decrease in the concentration of MO1 from 20.0 to 1.0 mg/L had caused increase in the percentage mineralisation of MO1 from 7.72 to 27.38% (for UV-A light) and from 4.12 to 17.1% (for LED light), respectively. The single reactor operation enabled to mineralise significantly

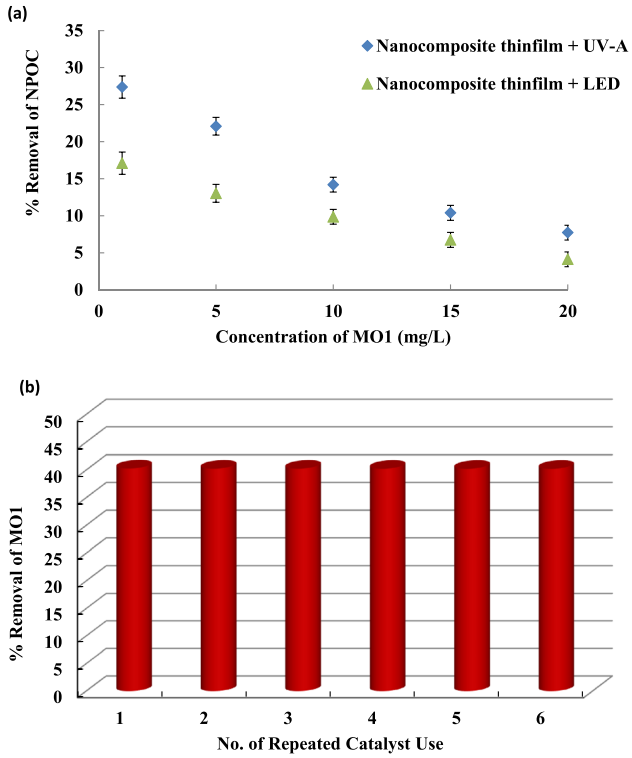

Fig. 4 **a** Percentage mineralisation of MO1 as a function of MO1 concentrations under the photocatalytic processes and **b** elimination efficiency of MO1 after a repeated cycle of catalyst operations [pH of solution: 6.0]

the percentage mineralisation of MO1. These findings are similar to the concentration-dependent studies conducted previously in the removal of MO1. On the other hand, the photolysis using the UV-A or LED irradiations showed almost negligible degradation of MO1. Therefore, the photocatalytic operations favoured the mineralisation of MO1 using the nanocomposite thin film photocatalyst (Tiwari et al. 2015).

Repetitive use of thin-film photocatalysts

The efficiency of the photocatalyst largely depends on its reusability for successive reactor operations. This eventually provides the sustainability of reactor operations and the cost-effectiveness of the process. Therefore, the reusability of nanocomposite thin film photocatalyst is carried out for repeated reactor operations in the elimination of MO1 (MO1 concentration: 5.0 mg/L; pH 6.0). The percentage elimination of MO1 with an effect of the number of cycles of reactor operations is shown in Fig. 4b. The degradation efficiency of the photocatalyst is almost unaffected even at the end of six successive cycles of reactor operations. Quantitatively, the percentage degradation of MO1 is decreased only from 40.29 to 40.23% (i.e. 0.06%). The results showed that the thin-film catalyst is reasonably stable towards the reactor operations in the photocatalytic degradation of MO1. Hence, the photocatalyst is shown to be employed for prolonged and sustainable operations. The successive implications of thin-film catalysts without losing their efficiency, at least in the removal of MO1, further indicated the greater applicability of solid with cost-effectiveness. Moreover, the results have shown that the materials are intact on the surface of borosilicate glass which is possibly due to the use of polyethylene glycol which enhances the mechanical strength of materials and prevented the leaching of TiO_2 in the solution (Rtimi et al. 2013).

Simultaneous presence of co-ions

Applicability of thin-film catalysts is further assessed in the presence of a variety of co-ions viz., glycine, oxalic acid, $NaNO_3$, NaCl, $CuSO_4$, $NiCl_2$, and EDTA. The initial concentrations of MO1 and coexisting ions were taken as 5.0 mg/L and 50.0 mg/L, respectively (pH 6.0 and UV-A illumination for 2 h). The removal efficiency of MO1 for the simultaneous presence of co-ions is shown in Fig. 5a. The removal efficiency of MO1 is affected by NaCl, EDTA, and glycine. However, the other ions introduced have not affected significantly the degradation of MO1 in the photocatalytic reactor operations. These results showed the potential of thin-film catalysts in the elimination of MO1 from aqueous solutions.

Degradation mechanism

It is known that the photons carrying enough energy ($h\upsilon$) may generate electron and hole pairs $e^- - h^+$ (Selvaraj and Li 2006). However, titanium dioxide possessed a wide bandgap energy (3.2 eV) hence, excited by the photons at the UV region only. However, the doping of titanium dioxide by noble metal (Ag(NP)) or Au(NP)) lowers apparent bandgap energy. Noble metal nanoparticles generate a phenomenon called localised surface plasmon resonance which enables TiO_2 photocatalyst to absorb light within the visible region and enhances the photo-excitation of electrons (Zangeneh et al. 2015). It also traps the newly generated electrons thus helping in reducing the charge recombination rate and allowing it to proceed further for photocatalytic reaction. Therefore, in order to demonstrate the possible mechanism involved in the elimination of MO1 using the nanocomposite photocatalyst, the investigation was extended in presence of several scavengers. 2-Propanol and HCO_3^- compounds are known $^{\bullet}OH$ radical scavengers (Xu et al. 2015; Lalhriatpuia et al. 2016); whereas EDTA scavenges the h^+ of photocatalyst (Jia et al. 2016). Similarly, the sodium azide traps singlet oxygen which is generated in reaction of $O_2^{-\bullet}$ with h^+ (Xu et al. 2015). Thus, the degradation of MO1 (5.0 mg/L; pH 6.0) in the presence of these scavengers is carried out using UV-A irradiation for 2 h. The degradation efficiency of MO1 is shown in Fig. 5b. The results inferred that the 2-propanol, HCO_3^-, and sodium azide greatly hampered the percentage degradation of MO1. This indicated that hydroxyl radicals are primarily involved in the degradation process. A sharp drop in the photocatalytic degradation of oxolinic acid (OA) using TiO_2/cellulosic paper catalysts due to the presence of 2-propanol and EDTA was also reported (Zeghioud et al. 2019). Additionally, NaN_3 suppressed the removal efficiency of MO1 and inferred that singlet oxygen is taking part in photocatalytic degradation reactions. Hence, it infers that the elimination mechanism of MO1 proceeds in two different possible pathways. First, the Ag(NPs) traps the newly generated electrons which help in inhibiting the charge recombination and allow it to go further for reaction to form peroxide radical and hydroxyl radicals (Ahmad et al. 2016). Peroxide radicals are generated at the conduction band through the interaction of trapped electrons and oxygen in the presence of water, while hydroxyl radicals are generated at the valence band through the interaction of the H_2O and oxygen (Akpan and Hameed 2009). Both the radicals then interacted with the pollutant at the vicinity of the thin film photocatalyst which results in the degradation of MO1 as shown in Fig. 5c (Vogna et al. 2004; Tiwari et al. 2019). The other possible pathway is that Ag(NPs) absorbs light radiations resulting in the generation of the electromagnetic field as because of localised surface plasmon resonance (Lee et al. 2014). Further, Schottky barrier

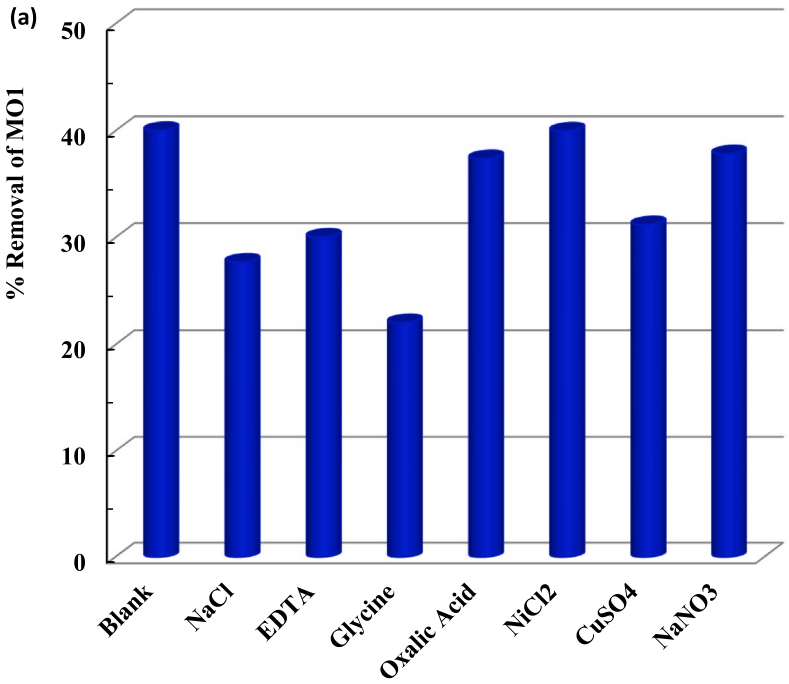
(a)
% Removal of MO1
50
40
30
20
10
0
Blank
NaCl
EDTA
Glycine
Oxalic Acid
NiCl2
CuSO4
NaNO3

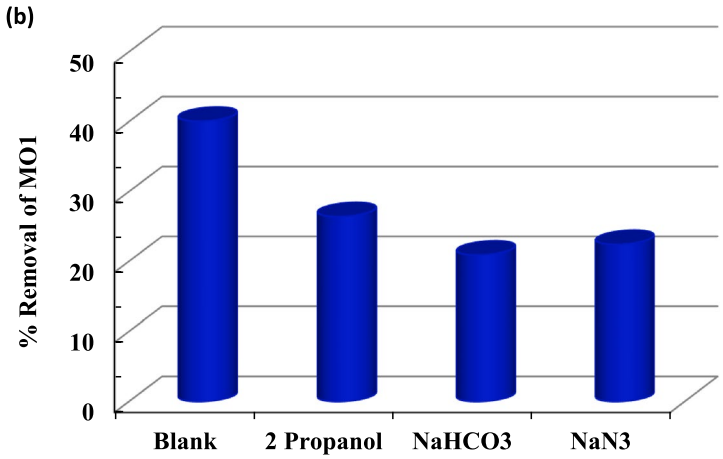
(b)
% Removal of MO1
50
40
30
20
10
0
Blank
2 Propanol
NaHCO3
NaN3

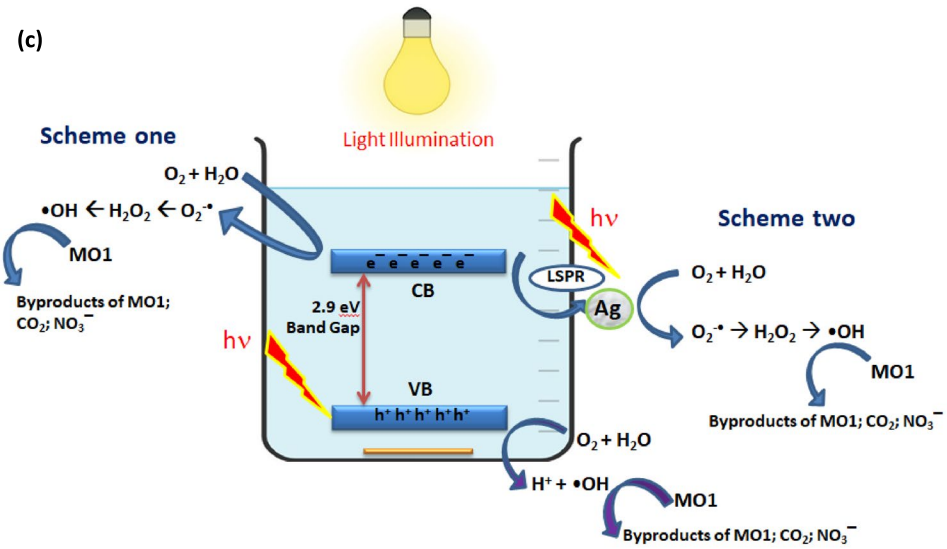
(c)
Scheme one
Light Illumination
O2 + H2O
•OH ← H2O2 ← O2-•
MO1
Byproducts of MO1; CO2; NO3−
hν
e− e− e− e− e−
CB
2.9 eV
Band Gap
VB
h+ h+ h+ h+ h+
hν
LSPR
Ag
Scheme two
O2 + H2O
O2-• → H2O2 → •OH
MO1
Byproducts of MO1; CO2; NO3−
O2 + H2O
H+ + •OH
MO1
Byproducts of MO1; CO2; NO3−

◂**Fig. 5** Photocatalytic elimination of MO1 with effect of **a** several coexisting ions [concentration of MO1: 5.0 mg/L; concentration of coexisting ions: 50.0 mg/L; pH:6.0]; **b** several scavengers [concentration of MO1: 5.0 mg/L; concentration of scavengers: 500.0 mg/L; pH:6.0]; and **c** schematic of the photocatalytic degradation of MO1 using Ag^0(NPs)/TiO_2 thin film

present with metal–semiconductor causes the excited electrons to move towards the electric field and the holes towards the opposite direction of the electric field. This inhibits the recombination of electron–hole pairs (Z et al. 2014). Further, the electron–hole pairs undergo further reaction to form peroxide radical and hydroxyl radical which take part in the degradation of MO1 (cf Fig. 5c).

Real water treatment

Applicability of fabricated nano catalyst depends greatly on its utility to real water samples. Hence, the intended performance of nano catalyst thin films in the elimination of MO1 was performed using the MO1-tagged real water samples. The physicochemical parameters are obtained for river water samples and is shown in Table 2. The real water was contained with high concentrations of Fe, Ca, and Zn. On the other hand, the TOC data showed that real water was contained with a high inorganic carbon value with less NPOC value. MO1 was tagged with real water having

Table 2 Various physicochemical parametric analysis of the Reiek Kai site, Tlawng River water

Parameters studied	Analytical results
pH	7.6
Conductivity	0.0172 S/m
Resistivity	0.0138 Mohm.cm
Salinity	0.12 PSU
Ox. red. potential	210.7 mV
Elements studied (AAS)	**(mg/L)**
Ni	0.0
Zn	0.535
Pb	0.078
Mn	0.01
Fe	0.198
Ca	2.341
Cu	0.0
TOC analysis	**(mg/L)**
Inorganic carbon	13.94
NPOC	2.493
Anions studied	**(mg/L)**
Nitrate	11.43
Fluoride	0.0
Sulphate	6.12
Phosphate	0.09

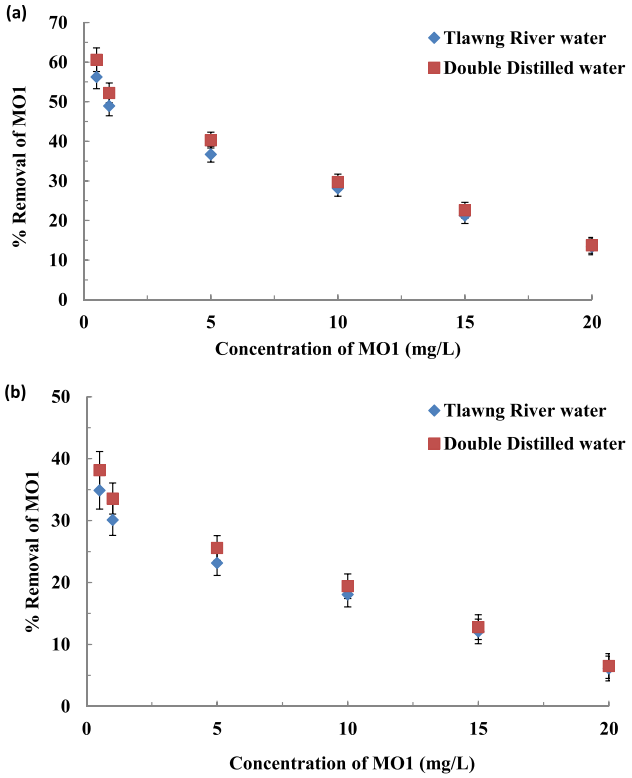

Fig. 6 Photocatalytic elimination of MO1 in distilled water and Tlawng River water using the nanocomposite thin film catalyst under **a** UV-A and **b** LED light

various concentrations of MO1 (0.5 to 20.0 mg/L; pH 6.0). Further, the degradative removal of MO1 is carried out using a nanocomposite thin film catalyst under UV-A and LED light illuminations for 2 h. Percentage degradation of MO1 was obtained and compared with the result obtained with the purified water samples (cf Fig. 6). The study revealed that the percentage degradation of MO1 was not significantly decreased in real water samples. This signifies the high applicability of nanocomposite thin film catalysts in the removal of MO1.

Conclusion

Nanocomposite (Ag^0(NPs)/TiO_2) is obtained using the facile template process. The thin film catalyst was fabricated by the dip-coating process. SEM images showed Ag is successfully doped uniformly within the titania network, and the interplanar distance of Ag^0(NPs) was 0.15 nm. AFM analyses showed that the root mean square roughness (R_q) and mean roughness (R_a) of the thin-film catalyst was 16.952 nm and 12.250 nm, respectively. The thin-film catalyst was utilised for the elimination of Mordant Orange-1 using UV-A and LED light irradiations. Lower pH values and lower

concentrations of MO1 have favoured greatly the removal efficiency of MO1. The increase in MO1 concentration from 0.5 to 20.0 mg/L had caused to decrease the percentage removal of MO1 from 60.61 to 13.74% and 38.14 to 6.5% under UV-A and LED irradiation, respectively. The photocatalytic elimination of MO1 has proceeded through pseudo-first-order rate kinetics. Moreover, a partial but significant amount of MO1 was mineralised by a single operation indicated greater applicability of photocatalytic process. With the increase in MO1 concentration from 1.0 to 20.0 mg/L, the percentage mineralisation of MO1 was decreased from 27.38 to 7.72% (for UV-A light) and from 17.1 to 4.12% (for LED light), respectively. Further, the presence of NaCl, EDTA, and glycine greatly influenced the degradation efficacy of the thin films. However, the other ions were not significantly affected by the removal efficiency of MO1. The scavenger studies indicated that the degradation of MO1 is primarily due to the reactive hydroxyl radicals, holes, and singlet oxygen which are primarily involved in the surface excitations. Moreover, the repetitive use of thin film catalysts showed almost no suppression in photocatalytic efficiency of thin film; hence, the nanocomposite thin films possess greater applicability in sustained reactor operations. Additionally, the real matrix operations using the Reiek Kai site, Tlawng River, Aizawl (India) water showed almost a similar removal efficiency compared to the distilled water treatment. The photocatalytic degradation of MO1 using the thin film catalyst (Ag^0(NPs)/TiO_2) was found to be sustainable and, perhaps, cost-effective in greater real matrix implications.

Author contribution CV conducted the basic experiments relating to photocatalytic reactor operations. CL fabricated the thin film samples and helped in compiling the data. DT has formulated the problem and finalised the manuscript. DJK has helped in drafting the paper and made corrections in the final paper.

Availability of data and materials The datasets used and/or analysed during the current study are available from the corresponding author on reasonable request.

Declarations

Ethics approval and consent to participate Not applicable.

Consent for publication Not applicable.

Competing interests The authors declare no competing interests.

References

Abdel-Messih MF, Ahmed MA, El-Sayed AS (2013) Photocatalytic decolorization of Rhodamine B dye using novel mesoporous SnO2–TiO2 nano mixed oxides prepared by sol–gel method. J Photochem Photobiol Chem 260:1–8. https://doi.org/10.1016/j.jphotochem.2013.03.011

Acosta-Esparza MA, Rivera LP, Pérez-Centeno A et al (2020) UV and Visible light photodegradation of methylene blue with graphene decorated titanium dioxide. Mater Res Express 7:035504. https://doi.org/10.1088/2053-1591/ab7ac5

Ahmad R, Ahmad Z, Khan A et al (2016) Photocatalytic systems as an advanced environmental remediation: recent developments, limitations and new avenues for applications. J Environ Chem Eng 4:4143–4164. https://doi.org/10.1016/j.jece.2016.09.009

Ajmal A, Majeed I, Malik R et al (2016) Photocatalytic degradation of textile dyes on Cu2O-CuO/TiO2 anatase powders. J Environ Chem Eng 4https://doi.org/10.1016/j.jece.2016.03.041

Akpan UG, Hameed BH (2009) Parameters affecting the photocatalytic degradation of dyes using TiO2-based photocatalysts: a review. J Hazard Mater 170:520–529. https://doi.org/10.1016/j.jhazmat.2009.05.039

Alves de Lima RO, Bazo AP, Salvadori DMF et al (2007) Mutagenic and carcinogenic potential of a textile azo dye processing plant effluent that impacts a drinking water source. Mutat Res 626:53–60. https://doi.org/10.1016/j.mrgentox.2006.08.002

Ge L, Xu M, Fang H (2006) Preparation and characterization of silver and indium vanadate co-doped TiO2 thin films as visible-light-activated photocatalyst. J Sol-Gel Sci Technol 40:65–73. https://doi.org/10.1007/s10971-006-8457-9

Gracia-Lor E, Sancho JV, Serrano R, Hernández F (2012) Occurrence and removal of pharmaceuticals in wastewater treatment plants at the Spanish Mediterranean area of Valencia. Chemosphere 87:453–462. https://doi.org/10.1016/j.chemosphere.2011.12.025

Gupta VK, Suhas, (2009) Application of low-cost adsorbents for dye removal – a review. J Environ Manage 90:2313–2342. https://doi.org/10.1016/j.jenvman.2008.11.017

H S, H K, M S-N, S M-D (2017) Enhanced photocatalytic degradation of dyes over graphene/Pd/TiO2 nanocomposites: TiO2 nanowires versus TiO2 nanoparticles. J Colloid Interface Sci 498:423-432https://doi.org/10.1016/j.jcis.2017.03.078

Hai F, Yamamoto K, Fukushi K (2007) Hybrid treatment systems for dye wastewater. Fac Sci - Pap Arch. https://doi.org/10.1080/10643380601174723

Hajjaji A, Elabidi M, Trabelsi K et al (2018) Bacterial adhesion and inactivation on Ag decorated TiO2-nanotubes under visible light: effect of the nanotubes geometry on the photocatalytic activity. Colloids Surf B Biointerfaces 170:92–98. https://doi.org/10.1016/j.colsurfb.2018.06.005

Hatch KL, Maibach HI (1995) Textile dye dermatitis. J Am Acad Dermatol 32:631–639. https://doi.org/10.1016/0190-9622(95)90350-x

Hichem Z, Khellaf N, Amrane A et al (2017) Photocatalytic performance of TiO2 impregnated polyester for the degradation of Reactive Green 12: implications of the surface pretreatment and the microstructure. J Photochem Photobiol Chem 346https://doi.org/10.1016/j.jphotochem.2017.07.005

Husain Q (2006) Potential applications of the oxidoreductive enzymes in the decolorization and detoxification of textile and other synthetic dyes from polluted water: a review. Crit Rev Biotechnol 26:201–221. https://doi.org/10.1080/07388550600969936

Jia Y, Liu J, Cha S et al (2016) Magnetically separable Au-TiO2/nanocube ZnFe2O4 composite for chlortetracycline removal in wastewater under visible light. J Ind Eng Chem 47https://doi.org/10.1016/j.jiec.2016.12.001

Jin X-C, Liu G-Q, Xu Z-H, Tao W-Y (2007) Decolorization of a dye industry effluent by Aspergillus fumigatus XC6. Appl Microbiol Biotechnol 74:239–243. https://doi.org/10.1007/s00253-006-0658-1

Jung K-W, Choi BH, Hwang M-J et al (2016) Fabrication of granular activated carbons derived from spent coffee grounds by entrapment in calcium alginate beads for adsorption of acid orange 7 and methylene blue. Bioresour Technol 219:185–195. https://doi.org/10.1016/j.biortech.2016.07.098

Krasner SW, Westerhoff P, Chen B et al (2009) Occurrence of disinfection byproducts in United States wastewater treatment plant effluents. Environ Sci Technol 43:8320–8325. https://doi.org/10.1021/es901611m

Kuppusamy S, Kadiyala V, Palanisami T et al (2017) Quercus robur acorn peel as a novel coagulating adsorbent for cationic dye removal from aquatic ecosystems. Ecol Eng 101:3–8. https://doi.org/10.1016/j.ecoleng.2017.01.014

Lalhriatpuia C, Tiwari A, Shukla A et al (2016) Nanopillars TiO2 thin film photocatalyst application in the remediation of aquatic environment. Korean J Chem Eng 33:3367–3373. https://doi.org/10.1007/s11814-016-0191-6

Lalhriatpuia C, Tiwari D, Tiwari A, Lee S-M (2015) Immobilized Nanopillars-TiO2 in the efficient removal of micro-pollutants from aqueous solutions: physico-chemical studies. Chem Eng J 281:782–792. https://doi.org/10.1016/j.cej.2015.07.032

Lalliansanga TD, Tiwari A et al (2019) Facile synthesis and characterization of nanocomposite Au0(NPs)/titanium dioxide: photocatalytic degradation of Alizarin Yellow. J Ind Eng Chem 82https://doi.org/10.1016/j.jiec.2019.10.008

Lee H, Lee YK, Hwang E, Park JY (2014) Enhanced surface plasmon effect of Ag/TiO2 nanodiodes on internal photoemission. J Phys Chem C 118:5650–5656. https://doi.org/10.1021/jp409894b

Lee YH, Matthews RD, Pavlostathis SG (2006) Biological decolorization of reactive anthraquinone and phthalocyanine dyes under various oxidation-reduction conditions. Water Environ Res Res Publ Water Environ Fed 78:156–169. https://doi.org/10.2175/106143005x89616

Li C, Lou T, Yan X et al (2018) Fabrication of pure chitosan nanofibrous membranes as effective absorbent for dye removal. Int J Biol Macromol 106:768–774. https://doi.org/10.1016/j.ijbiomac.2017.08.072

Li H, Liu S, Zhao J, Feng N (2016) Removal of reactive dyes from wastewater assisted with kaolin clay by magnesium hydroxide coagulation process A physicochemical and engineering aspects

Liu C, Lei Z, Yang Y et al (2013) Improvement in settleability and dewaterability of waste activated sludge by solar photocatalytic treatment in Ag/TiO2-coated glass tubular reactor. Bioresour Technol 137:57–62. https://doi.org/10.1016/j.biortech.2013.03.071

Matouq M, Al-Anber Z, Susumu N, et al (2014) The kinetic of dyes degradation resulted from food industry in wastewater using high frequency of ultrasound. Sep Purif Technol C:42–47. https://doi.org/10.1016/j.seppur.2014.08.002

Milosevic I. Jayaprakash A, Greenwood B et al (2017) Synergistic effect of fluorinated and N doped TiO2 nanoparticles leading to different microstructure and enhanced photocatalytic bacterial inactivation. Nanomaterials 7https://doi.org/10.3390/nano7110391

Milošević I, Rtimi S, Jayaprakash A et al (2018) Synthesis and characterization of fluorinated anatase nanoparticles and subsequent N-doping for efficient visible light activated photocatalysis. Colloids Surf B Biointerfaces 171:445–450. https://doi.org/10.1016/j.colsurfb.2018.07.035

Mogal S, Gandhi G, Mishra M et al (2014) Single-step synthesis of silver-doped titanium dioxide: influence of silver on structural, textural, and photocatalytic properties. Ind Eng Chem Res 53:5749–5758. https://doi.org/10.1021/ie404230q

MuhdJulkapli N, Bagheri S, Bee Abd Hamid S (2014) Recent advances in heterogeneous photocatalytic decolorization of synthetic dyes. Sci World J 2014:e692307. https://doi.org/10.1155/2014/692307

Nasseri S, Mahvi AH, Seyedsalehi M et al (2017) Degradation kinetics of tetracycline in aqueous solutions using peroxydisulfate activated by ultrasound irradiation: effect of radical scavenger and water matrix. J Mol Liq 241:704–714. https://doi.org/10.1016/j.molliq.2017.05.137

Nazar MF, Shah SS, Khosa MA (2010) Interaction of azo dye with cationic surfactant under different pH conditions. J Surfactants Deterg 13:529–537. https://doi.org/10.1007/s11743-009-1177-8

Papić S, Koprivanac N, Božić AL, Meteš A (2004) Removal of some reactive dyes from synthetic wastewater by combined Al(III) coagulation/carbon adsorption process. Dyes Pigments 3:291–298. https://doi.org/10.1016/S0143-7208(03)00148-7

Paz A, Carballo J, Pérez MJ, Domínguez JM (2017) Biological treatment of model dyes and textile wastewaters. Chemosphere 181:168–177. https://doi.org/10.1016/j.chemosphere.2017.04.046

Rashid MU, Bhuiyan MKH, Quayum ME (2013) Synthesis of silver nano particles (Ag-NPs) and their uses for quantitative analysis of vitamin C tablets. Dhaka Univ J Pharm Sci 12:29

Riera-Torres M, Gutiérrez-Bouzán C, Crespi M (2010) Combination of coagulation–flocculation and nanofiltration techniques for dye removal and water reuse in textile effluents. Desalination 252:53–59. https://doi.org/10.1016/j.desal.2009.11.002

Rosu M-C, Coros M, Pogacean F et al (2017) Azo dyes degradation using TiO2-Pt/graphene oxide and TiO2-Pt/reduced graphene oxide photocatalysts under UV and natural sunlight irradiation. Solid State Sci 70:13–20. https://doi.org/10.1016/j.solidstatesciences.2017.05.013

Rtimi S, Pulgarin C, Sanjines R, Kiwi J (2013) Innovative semi-transparent nanocomposite films presenting photo-switchable behavior and leading to a reduction of the risk of infection under sunlight. RSC Adv 3:16345–16348. https://doi.org/10.1039/C3RA42762E

Sadeghzade-Attar A (2018) Efficient photocatalytic degradation of methylene blue dye by SnO2 nanotubes synthesized at different calcination temperatures. Sol Energy Mater Sol Cells 183:16–24. https://doi.org/10.1016/j.solmat.2018.03.046

Salama A (2017) New sustainable hybrid material as adsorbent for dye removal from aqueous solutions. J Colloid Interface Sci 487:348–353. https://doi.org/10.1016/j.jcis.2016.10.034

Sangiorgi N, Aversa L, Tatti R et al (2017) Spectrophotometric method for optical band gap and electronic transitions determination of semiconductor materials. Opt Mater 64:18–25. https://doi.org/10.1016/j.optmat.2016.11.014

Schwarze M, Gross MA, Ebraheme A et al (2017) Biopolymers for dye removal via foam separation. Sep Purif Technol 188https://doi.org/10.1016/j.seppur.2017.07.025

Selvaraj R, Li X (2006) Enhanced photocatalytic activity of TiO2 by doping with Ag for degradation of 2,4,6-trichlorophenol in aqueous suspension. J Mol Catal Chem 243https://doi.org/10.1016/j.molcata.2005.08.010

Shen L, Jin Z, Wang D et al (2018) Enhance wastewater biological treatment through the bacteria induced graphene oxide hydrogel. Chemosphere 190:201–210. https://doi.org/10.1016/j.chemosphere.2017.09.105

Shi B, Li G, Wang D et al (2007) Removal of direct dyes by coagulation: the performance of preformed polymeric aluminum species. J Hazard Mater 143:567–574. https://doi.org/10.1016/j.jhazmat.2006.09.076

Shokri M, Jodat A, Modirshahla N, Behnajady M (2013) Photocatalytic degradation of chloramphenicol in an aqueous suspension of silver-doped TiO2 nanoparticles. Environ Technol 34:1161–1166. https://doi.org/10.1080/09593330.2012.743589

Sofianos MV, Boukos N, Vaimakis T, Trapalis C (2014) Decoration of TiO2 anatase nanoplates with silver nanoparticles on the 1 0 1 crystal facets and their photocatalytic behaviour. Appl Catal B Environ s 158–159:91–95. https://doi.org/10.1016/j.apcatb.2014.02.030

Su C-C, Pukdee-Asa M, Ratanatamskul C, Lu M-C (2011) Effect of operating parameters on decolorization and COD removal of three reactive dyes by Fenton's reagent using fluidized-bed reactor. Desalination 278:211–218. https://doi.org/10.1016/j.desal.2011.05.022

Tiwari A, Shukla A, Lalliansanga, et al (2019) Au-nanoparticle/nanopillars TiO2 meso-porous thin films in the degradation of tetracycline using UV-A light. J Ind Eng Chem 69:141–152. https://doi.org/10.1016/j.jiec.2018.09.027

Tiwari A, Shukla A, Lalliansanga null, et al (2018) Nanocomposite thin films Ag0(NP)/TiO2 in the efficient removal of micro-pollutants from aqueous solutions: a case study of tetracycline and sulfamethoxazole removal. J Environ Manage 220:96–108. https://doi.org/10.1016/j.jenvman.2018.05.019

Tiwari A, Shukla A, Lalliansanga null, et al (2020) Synthesis and characterization of Ag0(NPs)/TiO2 nanocomposite: insight studies of triclosan removal from aqueous solutions. Environ Technol 41:3500–3514. https://doi.org/10.1080/09593330.2019.1615127

Tiwari D, Lalhriatpuia C, Lalhmunsiama L et al (2015) Efficient application of nano-TiO2 thin films in the photocatalytic removal of Alizarin Yellow from aqueous solutions. Appl Surf Sci 353:275–283. https://doi.org/10.1016/j.apsusc.2015.06.131

Verma AK, Dash RR, Bhunia P (2012) A review on chemical coagulation/flocculation technologies for removal of colour from textile wastewaters. J Environ Manage 93:154–168. https://doi.org/10.1016/j.jenvman.2011.09.012

Vogna D, Marotta R, Napolitano A et al (2004) Advanced oxidation of the pharmaceutical drug diclofenac with UV/H2O2 and ozone. Water Res 38:414–422. https://doi.org/10.1016/j.watres.2003.09.028

Xu D, Liu K, Shi W, et al (2015) Ag-decorated K2Ta2O6 nanocomposite photocatalysts with enhanced visible-light-driven degradation activities of tetracycline (TC). Ceram Int 3 Part B:4444–4451. https://doi.org/10.1016/j.ceramint.2014.11.136

Yagub MT, Sen TK, Afroze S, Ang HM (2014) Dye and its removal from aqueous solution by adsorption: a review. Adv Colloid Interface Sci 209:172–184. https://doi.org/10.1016/j.cis.2014.04.002

Z C, S Z, H Q et al (2014) Preparation of visible-light nano-photocatalysts through decoration of TiO2 by silver nanoparticles in inverse miniemulsions. J Colloid Interface Sci 435:51-58https://doi.org/10.1016/j.jcis.2014.08.021

Zangeneh H, Zinatizadeh AAL, Habibi M et al (2015) Photocatalytic oxidation of organic dyes and pollutants in wastewater using different modified titanium dioxides: a comparative review. J Ind Eng Chem 26:1–36. https://doi.org/10.1016/j.jiec.2014.10.043

Zeghioud H, Kamagate M, Coulibaly LS et al (2019) Photocatalytic degradation of binary and ternary mixtures of antibiotics: reactive species investigation in pilot scale. Chem Eng Res Des 144:300–309. https://doi.org/10.1016/j.cherd.2019.02.015

Zhang J, Fu D, Xu Y, Liu C (2010) Optimization of parameters on photocatalytic degradation of chloramphenicol using TiO2 as photocatalyist by response surface methodology. J Environ Sci 22:1281–1289. https://doi.org/10.1016/S1001-0742(09)60251-5

Zucca P, Vinci C, Sollai F et al (2008) Degradation of Alizarin Red S under mild experimental conditions by immobilized 5,10,15,20-tetrakis(4-sulfonatophenyl)porphine–Mn(III) as a biomimetic peroxidase-like catalyst. J Mol Catal Chem 288:97–102. https://doi.org/10.1016/j.molcata.2008.04.001